IEEE INSTRUMENTATION & MEASUREMENT SOCIETY

Received 4 April 2023; revised 14 May 2023; accepted 15 May 2023. Date of publication 29 May 2023; date of current version 14 June 2023.
The review of this paper was arranged by Associate Editor Amitava Chatterjee.

Digital Object Identifier 10.1109/OJIM.2023.3280502

An Intelligent Food Salt Tester Using Cross-Conductive Sensor

SAYED AFZAL ALI [1] (Graduate Student Member, IEEE), MD. RAHAT MAHBOOB [1], AND TARIKUL ISLAM [2] (Senior Member, IEEE)

[1]Department of Electrical Engineering, School of Engineering, Tezpur University, Tezpur 784028, India

[2]Electrical Engineering Department, Jamia Millia Islamia University, New Delhi 110025, India

CORRESPONDING AUTHOR: T. ISLAM (e-mail: tislam@jmi.ac.in)

ABSTRACT Salt is a mineral used in various industries/foods to fulfil different needs. Its utilization for food preparation is most common and its unmonitored consumption leads to many diseases. In this article, two sensors S1 and S2 have been designed and simulated using COMSOL MULTIPHYSICS 5.6 software to measure the salt concentration of various salt samples. The performances of the sensor structure have been evaluated by varying geometrical parameters and electrode materials. The sensor works on the extension of Thompson and Lampard Theorem, a well-known principle used to fabricate a primary standard of capacitor. Sensor S2 is fabricated, and experiments are conducted with various concentrations of salt samples. The experimental results closely match the results of the simulation and the commercial conductivity meter. A highly linear response with a sensitivity of 1.87 mV/(mg/100 ml) and with an average repeatability index of $\pm 0.17\%$ is observed. Furthermore, the Gaussian Naïve Bayes-based machine learning algorithm has been used to categorize salt samples into eight different salt taste types. The data for salt concentration samples are generated using 100 volunteers. The machine learning algorithm achieved an accuracy of 93.33% for predicting salt taste type.

INDEX TERMS Circular structure, classification of salt samples, conductivity, four electrode, machine learning, salt taster.

I. INTRODUCTION

SALT is known for its utilization in different forms in industries, such as oil & gas, chemical, textile, metal, pharmaceutical, rubber, soap, water treatment, and for the preparation of food [1], [2], [3], [4], [5]. It consists of sodium molecules (40%) and chloride molecules (60%) [6]. Salt is commonly used as a universal taste enhancer and is consumed extensively across the world.

It also plays a crucial role in the proper functioning of our body. It contracts and relax muscles, conducts nerve impulse, and maintains the balance of water and minerals [6], [7]. Adult bodies require 5 g/day of salt as recommended by WHO [8], [9]. Therefore, higher salt intake could be harmful as it leads to many noncommunicable diseases (NCDs), such as cardiovascular diseases (CVDs), elevated blood pressure, hypertension, aggravation of asthma, chronic kidney disease, osteoporosis, stomach cancer, and many more [6], [10], [11], [12]. Chronic diseases, such as CVD, chronic respiratory disease, cancer, and diabetes contribute to 80% of deaths [13]. An inappropriate amount of salt in food many times leads to domestic violence [14]. Several studies have been conducted in line with the WHO Risk Assessment project [15] to understand the effect of salt consumption on human health. In these studies, reduced salt consumption was found to be beneficial for health [10], [16], [17], [18], [19].

The human body requires 2 g/day of sodium. The major portion of sodium ($\approx$ 90%) in our diet comes through salt intake and around 2.54 g of salt is equivalent to 1 g of sodium [20]. Our dietary food contains 15% of natural sodium, and 15%–20% sodium from cooking and eating whereas 70% directly comes through processed food [20], [21]. Hence, proper monitoring of salt in processed food as well as cooked food is crucial to reduce NCDs. Techniques used to measure the salt concentration

include computed tomography [22], [23], impedance spectroscopy [24], ion-selective electrode (ISE) [25], nanocomposite conductive sensors, and electrochemical sensors [26]. These techniques normally measure the conductivity of the salt sample and some of them are complex, require skilled manpower and the systems are not cost effective for the general use of a common man. The nanomaterials-based conductivity measurement system suffers from drift due to ageing and degradation of sensing film. Also, most of them do not use any machine learning tool for intelligent decision making in a user-friendly manner suitable for daily use.

However, in the measurement of conductivity for determining food quality, the salt concentration is of high interest because of its cost-effective nature, and simple integration and is applicable for solid foods too [27]. In a few reported works, conductivity has been utilized to measure salt content in cured ham [24], in-mouth salt release [28], blood [29], and water quality [30]. The work is limited by either using high-end technology or two electrodes technique.

Recently, the quality of bottled water and milk in terms of conductivity [31], [32] are being reported using cross structure. Therefore, a simple, low cost, and portable food salt tester with an intelligent decision-making system are required to measure the salt concentration in food and cuisine. Although the research is limited to a few, a detailed investigation through simulation and experiments to utilize the cross structure as a salt tester has not been yet reported.

In this work, a four electrode circular cross-sensor is proposed and investigated in detail as a salt tester. The sensor is based on a highly precise and accurate structure as proposed in the Thompson and Lampard (TL) theorem. The proposed sensor structure is initially designed in COMSOL MULTIPHYSICS 5.6 software. A detailed simulation study is being carried out to understand the sensor behavior for various design parameters and salt concentrations. The sensor is fabricated using inexpensive copper cladded PCB substrate and experiments are conducted with different salt samples in package drinking water to evaluate its static performance. Finally, Gaussian Naïve Bayes-based machine learning algorithm has been used to develop a decision-making system to indicate the presence of salt in water.

II. THEORETICAL BACKGROUND

The extension of the TL theorem offers a method for precise and accurate conductivity measurement [33]. A single-axis symmetry is the foundation of this approach. It gives a free hand to choose any suitable shape and structure as per requirement. To measure conductivity or capacitance the single axis of symmetry is a necessity irrespective of perfection. According to an extension of the TL theorem [34], the conductance value between an opposite pair of electrodes is known as the cross-conductance. The cross-conductance of a hollow circular structure with one axis of symmetry is proportional only to its single-dimensional electrode length.

The circular cross structure as shown in Fig. 1(a) consists of four electrodes labeled E_1, E_2, E_3, and E_4 having an

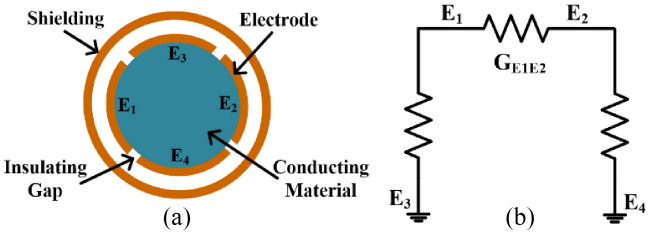

FIGURE 1. (a) Schematic of a circular cross sensor with shielding. (b) Equivalent electrical circuit of cross sensor with cross conductance.

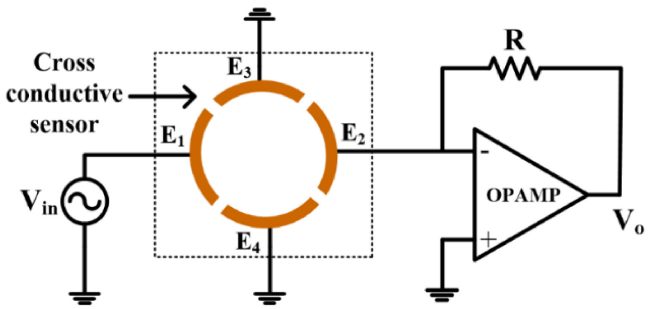

FIGURE 2. Interfacing circuit of the sensor.

equal gap between each pair of electrodes. The circular cross electrodes have been shielded using metal guards and its electrical equivalent model is shown in Fig. 1(b).

The conductivity for circular cross sensor governed by

$$\sigma = \frac{\pi G_0}{\ln 2} \tag{1}$$

where σ and G_o are material conductivity (material placed in a hollow section) and cross conductance per unit length [33]. The conductivity value can be measured by giving sinusoidal signals (V_{in}) at electrode E_1. The electrodes E_3 and E_4 are grounded while the cross conductance is measured between the electrodes E_1 and E_2. An interfacing circuit is connected at electrode E_2 which gives voltage corresponding to conductance value. The circuit comprises an inverting operational amplifier with R as feedback resistance as shown in Fig. 2.

The cross-resistance between the electrodes E_1-E_2, and E_3-E_4 are R_{E1E2} and R_{E3E4}, respectively. Therefore, the corresponding cross-conductance will be G_{E1E2} and G_{E3E4}

$$G_{E1E2} = \frac{1}{R_{E1E2}} \text{ and } G_{E3E4} = \frac{1}{R_{E3E4}}. \tag{2}$$

The output V_o of the OPAMP is

$$V_0 = \frac{-R}{R_{E1E2}} \times V_{\text{in}} = -R \times G_{E1E2} \times V_{\text{in}}. \tag{3}$$

As G_0 is cross-conductance per unit length therefore it could be written as

$$G_o = \frac{G_{E1E2}}{d} \tag{4}$$

where d is the thickness of the material/structure. Therefore, the output voltage as per (1), (3), and (4) is

$$V_0 = \frac{-\sigma R V_{\text{in}} (\ln 2)\, d}{\pi}. \tag{5}$$

Equation (5) gives the relationship between voltage and conductivity values. The relationship reveals that the output voltage depends only on the single variable parameter, thickness (d).

III. DESIGN AND SIMULATION

Two identical circular cross sensors were designed with and without shielding using the COMSOL MULTIPHYSICS 5.6 software [35]. The geometrical structure of the sensor was prepared using the "model builder section." The model builder facilities the option of adding geometry, material, and physics as per the requirement of the structure. The structure of the cross sensor was designed with geometrical parameters: an effective area of 200 mm^2, thickness of 1 mm, and 0.5-mm electrode gap. The material used for the electrode available in the material section was copper. Further from the physics section, in the ac/dc Module [36], the electric circuit and electric current modules were added to perform simulation of the interfacing circuit. The time-dependent study was conducted using "the study section." The sensor output voltage was obtained through global evaluation from the derived values in the result section.

An excitation signal with ±2-V amplitude at 1-kHz frequency was applied to the electrode E1, whereas the electrodes E3 and E4 were at ground potential. The sensor was excited by ac signal of suitable frequency to avoid the electrode's polarization. The simulation was conducted by varying signal frequency and amplitude. At low frequency, electromagnetic interference, particularly, the power frequency interference, influences the reading of the sensor. This interference is reduced at higher frequency so the relatively high frequency such as 1 kHz was selected. The interference can be further reduced at much higher frequency but at high frequency, the performance of the Opamp used for interfacing the circuit is also reduced. Therefore, 1-kHz frequency was found to be suitable for excitation. The output voltage of the interfacing circuit is directly proportional to the conductivity of the salt sample. So, to avoid Opamp output saturation, a low-amplitude ac signal was used. Therefore, the simulation and the experiment were performed at a low ac input voltage of 60 mV (RMS). The signal received at the electrode E2 was further conditioned using an interface circuit which gives the corresponding voltage output (Vo). The sensor was designed to keep the size of the sensor small so that a small amount of test sample is required for conductivity measurement. However, the geometrical parameters were optimized for better sensitivity. The materials were selected such that the sensor including the circuit can be fabricated at a low cost. A detailed investigation of the design criterion that includes the size of the sensor, the material of the electrode, the electrode gap, the thickness of the sensor, and the effect of shielding is reported in our recent work [38]. To keep the prototype system inexpensive, the sensor and the circuit were integrated on a copper cladded PCB. The sensor measured the conductivity of the material placed inside the four electrodes.

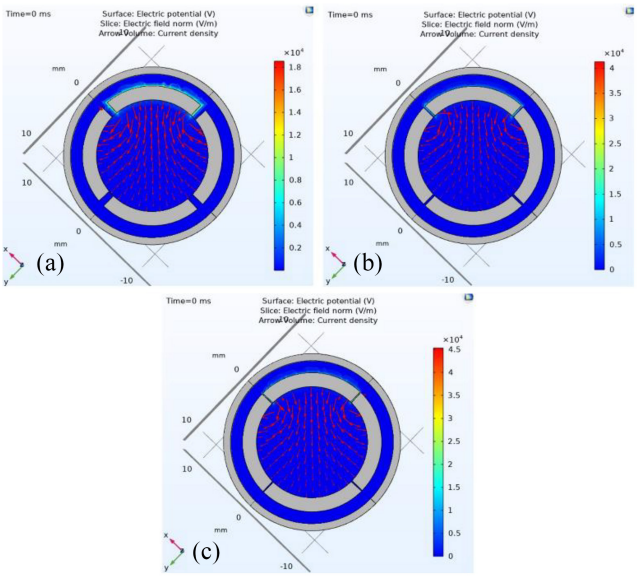

FIGURE 3. Electric field distribution with electrode gap. (a) 1 mm. (b) 0.5 mm. (c) 0.25 mm.

The placed material formed the conductance G_{E1E2} of the electrical equivalent circuit as shown in Fig. 1(b). The sensor was first simulated by placing a thin layer of water having a standard conductivity of 50 mS/m [37]. The output voltage obtained corresponding to sensors S1 and S2 were −220.53 and −220.63 mV, respectively. The conductivity was then calculated using (5). Sensor S1 yields a conductivity value of 49.95 mS/m with an error of 0.10% whereas sensor S2 results in only 0.06% error with respect to the standard conductivity value. The comparatively high error for sensor S1 is due to the fringing field effect which gets minimized in S2 through shielding [38]. Hence, sensor S2 structure was fabricated for experimental validation of the theory.

A simulation was performed on sensor S2 by varying the insulation gap between 0.25 and 1 mm. The electric field distribution profile of sensor S2 for different insulation gaps is shown in Fig. 3. The surface plot confirms the dependence of a smaller gap between the electrodes for establishing a stronger electric field with minimal fringing effect.

The distribution of the electric field and, thus, the sensitivity of the structure are significantly influenced by the insulating gap between the electrodes.

IV. SENSOR FABRICATION AND EXPERIMENTAL SETUP

The proposed sensor was fabricated using copper cladded glass fibre epoxy substrate in the lab. Constflick Technologies Limited, China, provided the glass fibre epoxy substrate (EC-9331). Four identical copper electrodes with an inner diameter of 4.5 mm, a track width of 2 mm, and insulating gaps of 0.25 mm were fabricated as shown in Fig. 4.

The undesirable copper was chemically removed through the etching process. The outer copper track acts as a guard electrode to provide shielding. An accurate hollow space with

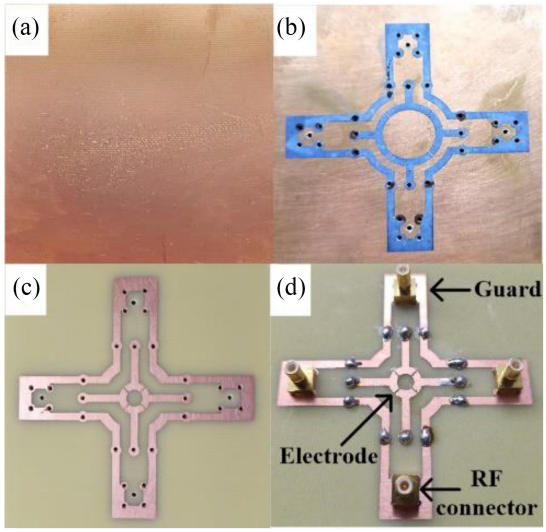

FIGURE 4. (a) Glass fibre epoxy substrate with copper. (b) Masked sensor structure. (c) Etched circular sensor. (d) Final sensor structure.

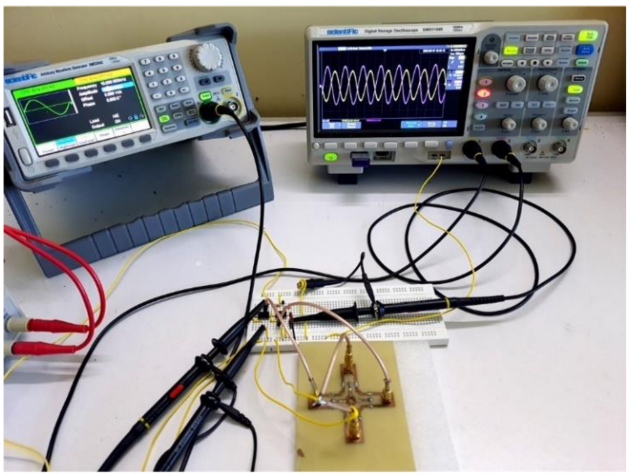

FIGURE 5. Sensor experimental set up with interfacing circuit.

a depth of 1.5 mm and a diameter of 4.5 mm was created at the center of the four electrodes to hold the sample.

An ac excitation signal of 61 mV (RMS) with a frequency of 10 kHz was applied using a function generator (SMG2042) to the electrode E_1. The electrodes E_3 and E_4 were kept grounded while the signal received at electrode E_2 was applied to the signal conditioning circuit. RF connector and shielded cables were used to reduce the effect of parasitic capacitances and noises as shown in Fig. 5. The signal conditioning circuit was made using an operational amplifier (LF356) and an RC low-pass filter. The output of the circuit was observed on a digital storage oscilloscope (SM01104E).

The sensor response was measured for different conductivity samples. Commercially available TATA salt was used for preparing 10 different salt samples having conductivity values varying from 12 to 6000 mS/m. The samples were labeled S_1, S_2, S_3 up to S_{10}. The samples were prepared by

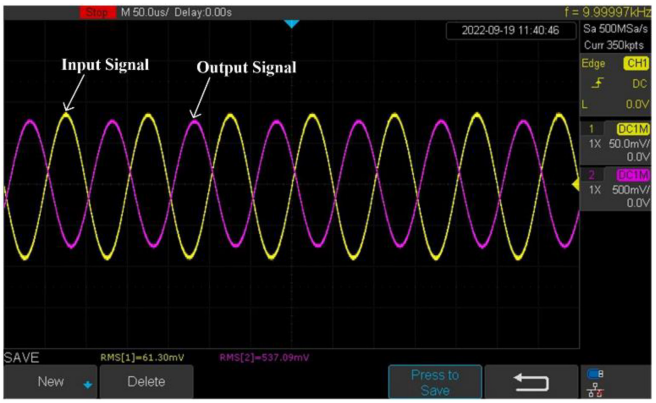

FIGURE 6. Signal waveform for sample S_2.

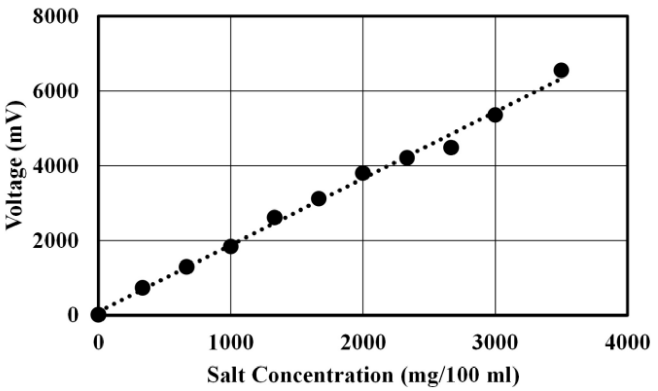

FIGURE 7. Sensor response curve with different salt samples.

mixing TATA salt of 0 mg, 100 mg, 200 mg up to 900 mg in 30 ml of package drinking water.

A fixed volume of each sample was placed in the space within the electrodes of the sensor using a micropipette (LHC37112020). However, the position of the droplet in the space may cause some errors in output voltage as reported in [39]. To ensure, identical droplet volume and its position, a hollow space at the center of the electrodes was created and the droplet was placed in the space only. All the experiments are performed at room temperature. The input and output waveforms obtained for sample S_2 are shown in Fig. 6. There is a change in the peak of the amplitude of the output signal due to placement of conductive sample.

The change in output voltage with the variation of salt concentration is shown in Fig. 7. The output voltage increases with an increase in salt concentration linearly from 0.0 to 3500 mg/100 ml with a resolution of 33 mg/100 ml. The sensitivity of the sensor output is ~2 mV/(mg/100 ml). The output signal can be easily scaled to a suitable level by using another stage of the amplifier.

V. MACHINE LEARNING ALGORITHM FOR SALT CATEGORIZATION

The proposed sensor is developed specifically to predict the amount of salt present in food. A detailed experiment was

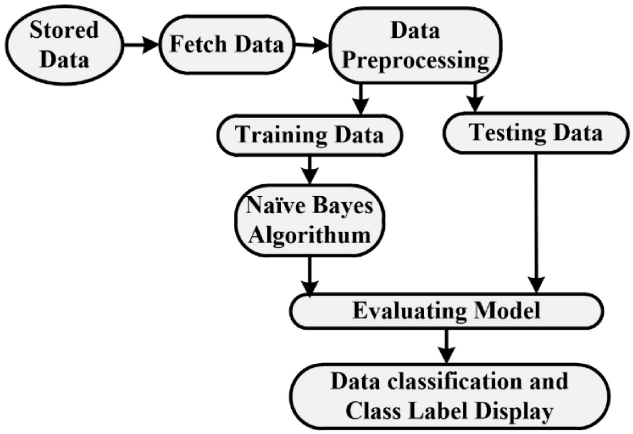

FIGURE 8. Proposed model for classification of salt taste type.

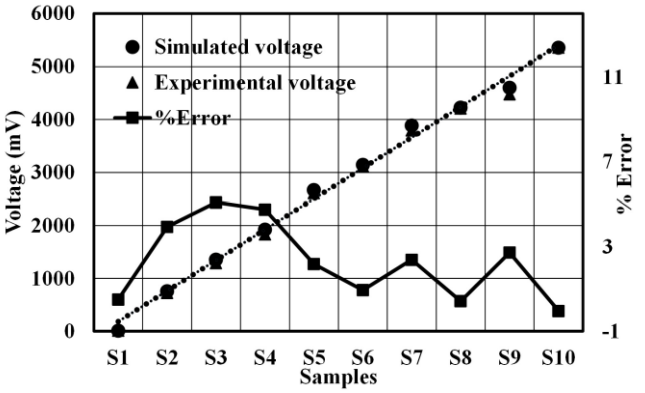

FIGURE 9. Experimental and simulated output voltage of sensor for different samples with its error.

TABLE 1. Conductivity comparison.

Sample Name	Salt (mg)	σ_{Meter} (mS/m)	$\sigma_{Simulated}$ (mS/m)	$\sigma_{Experimental}$ (mS/m)
S_1	0	12.72	12.72	12.65
S_2	100	824.00	825.18	792.69
S_3	200	1476.00	1480.04	1404.74
S_4	300	2090.00	2096.90	1997.16
S_5	400	2890.00	2906.67	2843.36
S_6	500	3420.00	3427.63	3395.15
S_7	600	4200.00	4237.40	4136.34
S_8	700	4600.00	4605.77	4586.07
S_9	800	4970.00	5015.56	4878.98
S_{10}	900	5830.00	5832.96	5835.09

conducted to make an intelligent decision about the presence of salt in food.

Volunteers in the age group of 20–30 years belonging to different geographical locations of India from two different universities were involved to test salt samples and were asked to give a decision in linguistic variables like very low salt, high salt, etc. The volunteers were selected based on region, culture, and food habits. To implement the Gaussian Naïve Bayes algorithm, a set of data have been collected using a prepared questionnaire. In our work, the data was limited to 100 volunteers only. The probabilistic classification model through a supervised learning technique called the Gaussian Naïve Bayes algorithm was implemented for the categorizing amount of salt. The Gaussian Naive Bayes algorithm is known to perform well on small to moderate-sized datasets. It is based on the Bayes theorem and models the probability distribution of each feature for each class using a Gaussian distribution and supports continuous data [40]. The algorithm selects the class with the highest probability as the predicted class for the data point. The flow chart of the proposed model for the classification of salt taste type is shown in Fig. 8.

For the survey, a series of samples with different unknown salt concentrations were prepared. To record the volunteer's responses, the prepared questionnaire containing linguistic identification of salt concentration was utilized. Eight different salt taste types were prepared and categorized as No salt (N), Extremely Low salt (EL), Very Low salt (VL), Low salt (L), Normal salt (NL), High salt (H), Very High salt (VH), and Extremely Highsalt (EH). To achieve uniformity and enhance the overall quality of data to improve the accuracy of the classifier, data preprocessing was done. The redundant data was filtered and processed. The processed data were grouped into a training dataset (70%) and a testing dataset (30%). The algorithm learns from training data sets and finds mapping between input and output that generates the model. The model was evaluated by using 30% testing dataset. To evaluate the performance and accuracy of the proposed machine learning model, a confusion matrix was calculated. Also, mean square error (MSE) and root MSE (RMSE) were calculated. The machine learning algorithm was written and executed using Colaboratory [41] (a product from Google Research).

VI. RESULT AND DISCUSSION

The working of the proposed salt testing sensor was first carried out through simulation and then established via experimental results. The physical dimension of the fabricated sensor and the sensor for simulation were the same. The comparison of the experimental data with simulation data is shown in Fig. 9. The sensor output voltage obtained experimentally is in good agreement with the simulated values. An average error of 2.3% with an average relative standard deviation (SD) of 1.7% was obtained. The error obtained in the experimental result is due to the limitation in the accuracy of sensor structure design through the chemical etching process.

To further examine the accuracy and performance of the proposed salt testing sensor, the obtained voltages corresponding to different salt samples have been converted to conductivity using (??). The samples conductivity was first measured using a commercially available conductivity meter EUTECH Instruments CON 700 and then was determined from the Vo of the sensor.

Table 1 shows the comparison of conductivity values of different samples compared with the simulated ($\sigma_{Simulated}$) and experimental ($\sigma_{Experimental}$).

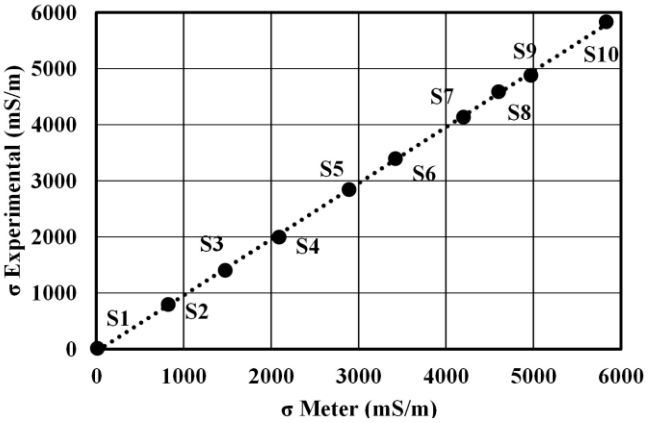

FIGURE 10. Sensor conductivity with reference to commercial conductivity meter.

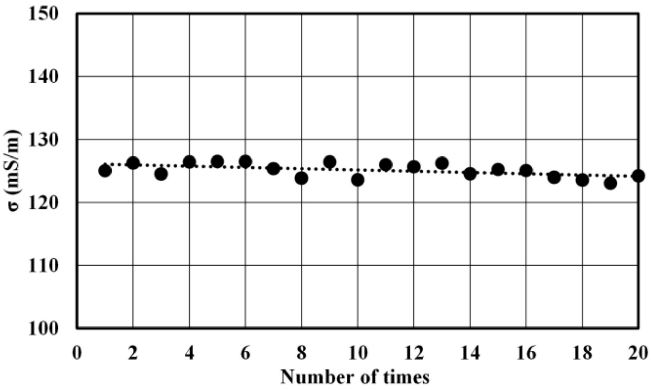

FIGURE 11. Repeatability curve of the sensor for 20 test samples of the same concentration.

Table 1 shows the effectiveness of the proposed salt tester for measuring conductivity. The average error is +1.95% as compared to a commercial meter having an accuracy of ± 1%. The calibration curve is shown in Fig. 10.

The precision of the sensor's reading was established by testing each salt sample 20 times to establish the proposed sensor. The time between two consecutive measurements was close to 2 min. While performing the repeatability test, necessary precautions were taken to ensure identical environmental conditions by keeping temperature and humidity constant as far as possible. After each measurement, the electrode was also properly cleaned. The sensor gave precise readings with an average repeatability index [42] of ±0.17%. Fig. 11 shows the repeatability curve of a random sample prepared with 10 mg TATA salt in 30 ml of package drinking water. The SD and the mean SD (SDM) are only 1.13 and 0.25, respectively.

The primary goal of the proposed work is to develop an intelligent salt tester to determine the salt concentration in the food. The survey results obtained in Section V were used to train the machine learning algorithm. The Gaussian Naïve Bayes classifier predicted salt taste types as indicated in Fig. 12 based on thorough training.

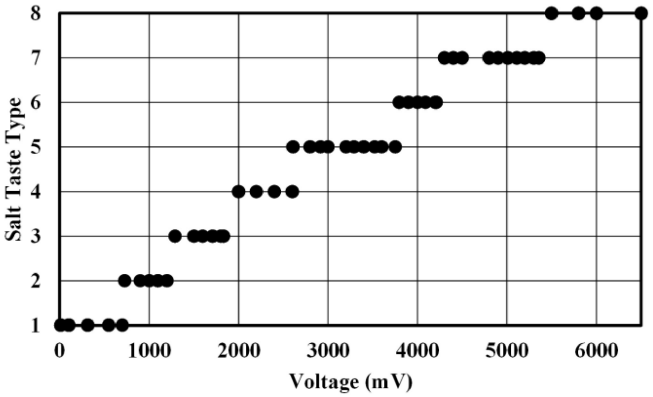

FIGURE 12. Predicted salt taste type by ML for 30%.

TABLE 2. ML predicted linguistic salt taste type.

Salt Taste Type	Linguistic Salt Tester	Conductivity (mS/m)
1	No Salt in water (N)	0-762.89
2	Extremely low salt (EL)	763.98-1416.81
3	Very low salt (VL)	1417.90-2016.24
4	Low salt (L)	2017.33-2833.63
5	Normal salt (NL)	2834.72-4141.46
6	High salt (H)	4142.55-4577.39
7	Very high salt (VH)	4578.49-5994.21
8	Extremely high salt (EH)	>5995.00

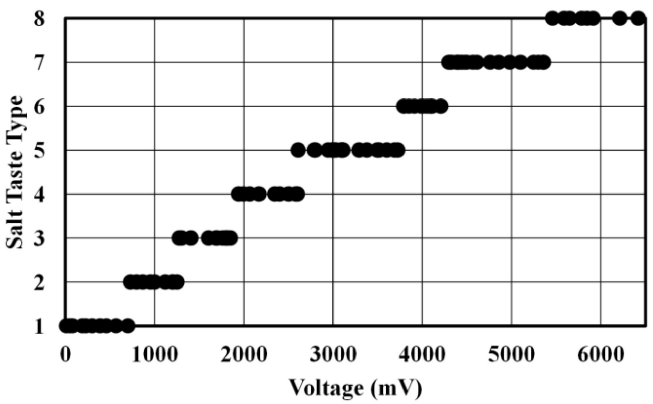

FIGURE 13. Salt taste type for random 100 salt solutions.

The accuracy of the predicted salt taste type was found to be 93.3%. It is calculated using a confusion matrix by taking the ratio of the total number of correct classifications to the total number of classifications. The MSE and RMSE were calculated and these are 0.07 and 0.26, respectively. An MSE value closer to zero indicates a good model.

The approximate interpretation of predicted results for salt taste type through ML in terms of conductivity is shown in Table 2.

The trained machine learning model was further tested for random 100 salt solutions. The classification of salt taste type is shown in Fig. 13 and found in accordance with the result obtained in Table 2.

The proposed structure has the potential to predict salt concentration in food. But initial experiments were conducted by measuring salt concentration in package drinking water. However, we have planned to conduct test to measure salt concentration in food such as in different varieties of "dal," a common food item in India. The detailed investigation will be reported as an extension of the present work in future.

VII. CONCLUSION

This work presents a four electrode food salt tester based on a cross-conductive circular structure. A detailed simulation on COMSOL suggested that sensor S2 is suitable for the development of the salt tester. Sensor S2 was fabricated and the experiment was conducted from 0.0 to 3500 mg/100 ml salt samples with a resolution of 33 mg/100 ml. The experimental results are found in accordance with the simulation results with a maximum average relative SD of 1.7%. The machine algorithm categorizes the conductivity in terms of salt taste type. The overall accuracy to categories the salt concentration is 93.3%. The accuracy could be further improved by increasing the dataset to train and test the proposed ML model. A simple sensor-based intelligent salt tester is developed to classify the salt amount in food for various applications.

ACKNOWLEDGMENT

The authors are thankful to AICTE for providing ADF scholarship and Tezpur University for Research TU/Fin/Conc./NR/2022-23/03300.

REFERENCES

[1] D. F. Williams and K. T. Clarno, "Evaluation of salt coolants for reactor applications," *Nucl. Technol.*, vol. 163, no. 3, pp. 330–343, Sep. 2008, doi: 10.13182/NT08-A3992.

[2] M. Círillo, G. Capasso, V. A. D. Leo, and N. G. D. Santo, "A history of salt," *Amer. J. Nurs.*, vol. 14, nos. 4–6, pp. 426–431, 1994, doi: 10.1159/000168759.

[3] M. Kare, *Biological and Behavioral Aspects of Salt Intake*. Burlington, MA, USA: Elsevier, 2012.

[4] M. S. Conner, "The uses of salt," *Obsidian*, vol. 41, nos. 1–2, pp. 177–190, 2015.

[5] M. Ruiz-Llata, P. Martín-Mateos, J. R. López, and P. Acedo, "Remote optical sensor for real-time residual salt monitoring on road surfaces," *Sens. Actuat. B, Chem.*, vol. 191, pp. 371–376, Feb. 2014, doi: 10.1016/j.snb.2013.10.009.

[6] E. Durack, M. Alonso-Gomez, and M. G. Wilkinson, "Salt: A review of its role in food science and public health," *Current Nutr. Food Sci.*, vol. 4, no. 4, pp. 290–297, Nov. 2008, doi: 10.2174/157340108786263702.

[7] M. Oria, M. Harrison, and V. A. Stallings, "National academies of sciences, engineering, and medicine; health and medicine division; food and nutrition board; committee to review the dietary reference intakes for sodium and potassium," in *Dietary Reference Intakes for Sodium and Potassium*, vol. 1. Washington, DC, USA: Nat. Acad. Press, 2019, pp. 1–10. [Online]. Available: http://www.ncbi.nlm.nih.gov/books/NBK538102

[8] J. G. Mill et al., "Estimation of salt intake in the Brazilian population: Results from the 2013 national health survey," *Rev. Bras. Epidemiol.*, vol. 22, Oct. 2019, Art. no. E190009, doi: 10.1590/1980-549720190009.supl.2.

[9] R. McLean, "Low sodium salt substitutes: A tool for sodium reduction and cardiovascular health," *Cochrane Database Syst. Rev.*, vol. 8, no. 8, 2022, Art. no. ED000158, doi: 10.1002/14651858.ED000158.

[10] I. J. Brown, I. Tzoulaki, V. Candeias, and P. Elliott, "Salt intakes around the world: Implications for public health," *Int. J. Epidemiol.*, vol. 38, no. 3, pp. 791–813, Jun. 2009, doi: 10.1093/ije/dyp139.

[11] T. A. Kotchen, A. W. Cowley, and E. D. Frohlich, "Salt in health and disease—A delicate balance," *New England J. Med.*, vol. 368, no. 13, pp. 1229–1237, Mar. 2013, doi: 10.1056/NEJMra1212606.

[12] X. Zhang, B. Chen, P. Jia, and J. Han, "Locked on salt? Excessive consumption of high-sodium foods during COVID-19 presents an underappreciated public health risk: A review," *Environ. Chem. Lett.*, vol. 19, no. 5, pp. 3583–3595, Oct. 2021, doi: 10.1007/s10311-021-01257-0.

[13] F. J. He, K. H. Jenner, and G. A. MacGregor, "WASH—World action on salt and health," *Kidney Int.*, vol. 78, no. 8, pp. 745–753, Oct. 2010, doi: 10.1038/ki.2010.280.

[14] S. Pengpid and K. Peltzer, "Associations of physical partner violence and sexual violence victimization on health risk behaviours and mental health among university students from 25 countries," *BMC Public Health*, vol. 20, no. 1, p. 937, Jul. 2020, doi: 10.1186/s12889-020-09064-y.

[15] M. Ezzati, A. D. Lopez, A. A. Rodgers, and C. J. L. Murray. "Comparative quantification of health risks: Global and regional burden of disease attributable to selected major risk factors." World Health Organization. 2004. Accessed: Feb. 26, 2023. [Online]. Available: https://apps.who.int/iris/handle/10665/42770

[16] P. Asaria, D. Chisholm, C. Mathers, M. Ezzati, and R. Beaglehole, "Chronic disease prevention: Health effects and financial costs of strategies to reduce salt intake and control tobacco use," *Lancet*, vol. 370, no. 9604, pp. 2044–2053, Dec. 2007, doi: 10.1016/S0140-6736(07)61698-5.

[17] F. J. He and G. A. MacGregor, "Effect of modest salt reduction on blood pressure: A meta-analysis of randomized trials. Implications for public health," *J. Human Hypertens.*, vol. 16, no. 11, pp. 761–770, Nov. 2002, doi: 10.1038/sj.jhh.1001459.

[18] F. J. He and G. A. MacGregor, "A comprehensive review on salt and health and current experience of worldwide salt reduction programmes," *J. Human Hypertens.*, vol. 23, no. 6, pp. 363–384, Jun. 2009, doi: 10.1038/jhh.2008.144.

[19] P. S. Sarma et al., "Prevalence of risk factors of non-communicable diseases in Kerala, India: Results of a cross-sectional study," *BMJ Open*, vol. 9, no. 11, Nov. 2019, Art. no. e027880, doi: 10.1136/bmjopen-2018-027880.

[20] "Salt and health: Review of the scientific evidence and recommendations for public policy in Ireland (revision 1)," Food Safety Authority of Ireland (FSAI), Dublin, Ireland, Rep., 2016. Accessed: Nov. 7, 2022. [Online]. Available: https://www.lenus.ie/handle/10147/609526

[21] "'SACN salt and health report': Recommendations on salt in diet." GOV.U.K. Accessed: Nov. 7, 2022. [Online]. Available: https://www.gov.uk/government/publications/sacn-salt-and-health-report

[22] C. Vestergaard, J. Risum, and J. Adler-Nissen, "Quantification of salt concentrations in cured pork by computed tomography," *Meat Sci.*, vol. 68, no. 1, pp. 107–113, Sep. 2004, doi: 10.1016/j.meatsci.2004.02.011.

[23] E. Fulladosa, E. Santos-Garcés, P. Picouet, and P. Gou, "Prediction of salt and water content in dry-cured hams by computed tomography," *J. Food Eng.*, vol. 96, no. 1, pp. 80–85, Jan. 2010, doi: 10.1016/j.jfoodeng.2009.06.044.

[24] R. Masot et al., "Design of a low-cost non-destructive system for punctual measurements of salt levels in food products using impedance spectroscopy," *Sens. Actuat. A, Phys.*, vol. 158, no. 2, pp. 217–223, Mar. 2010, doi: 10.1016/j.sna.2010.01.010.

[25] S. Woyesa, W. Gebisa, and D. L. Anshebo, "Assessment of selected serum electrolyte and associated risk factors in diabetic patients," *Diabetes Metab. Syndrome Obesity Targets Ther.*, vol. 12, pp. 2811–2817, Dec. 2019. [Online]. Available: https://www.semanticscholar.org/paper/Assessment-of-Selected-Serum-Electrolyte-and-Risk-Woyesa-Gebisa/bee11e0bfc3b7d004adb204054edbacf84a823e7

[26] K. L. Fukushima et al., "Development of an electronic tongue based on a nanocomposite for discriminating flavor enhancers and commercial salts," *IEEE Sensors J.*, vol. 21, no. 2, pp. 1250–1256, Jan. 2021, doi: 10.1109/JSEN.2020.3021653.

[27] E. García-Breijo et al., "Development of a puncture electronic device for electrical conductivity measurements throughout meat salting," *Sens. Actuat. A, Phys.*, vol. 148, no. 1, pp. 63–67, Nov. 2008, doi: 10.1016/j.sna.2008.07.013.

[28] M. Emorine, P. Mielle, J. Maratray, C. Septier, T. Thomas-Danguin, and C. Salles, "Use of sensors to measure in-mouth salt release during food chewing," *IEEE Sensors J.*, vol. 12, no. 11, pp. 3124–3130, Nov. 2012, doi: 10.1109/JSEN.2012.2215471.
[29] H. Ramaswamy, P. Prabhu, S. K. N. M. C, and S. Rajakannu, "Design and validation of a blood-salt level analysis meter," in *Proc. IEEE Delhi Section Conf. (DELCON)*, Feb. 2022, pp. 1–7, doi: 10.1109/DELCON54057.2022.9753648.
[30] A. F. Rusydi, "Correlation between conductivity and total dissolved solid in various type of water: A review," in *Proc. IOP Conf. Ser. Earth Environ. Sci.*, vol. 118, Feb. 2018, Art. no. 12019, doi: 10.1088/1755-1315/118/1/012019.
[31] T. Islam, A. Salamat, S. K. Singh, and M. Rehman, "A cross-conductive sensor to measure bottled water quality," in *Proc. IEEE Int. Instrum. Meas. Technol. Conf. (I2MTC)*, May 2021, pp. 1–6, doi: 10.1109/I2MTC50364.2021.9459929.
[32] T. Islam, A. Salamat, S. K. Singh, and M. Rehman, "A direct AC cross conductive sensor for milk quality measurement," *IEEE Trans. Instrum. Meas.*, vol. 71, pp. 1–8, 2022, doi: 10.1109/TIM.2022.3147313.
[33] A. M. Thompson and D. G. Lampard, "A new theorem in electrostatics and its application to calculable standards of capacitance," *Nature*, vol. 177, no. 4515, p. 887, May 1956, doi: 10.1038/177888a0.
[34] M. Rehman and V. G. K. Murti, "An extension and application of the Thompson–Lampard theorem," *Proc. IEEE*, vol. 69, no. 11, pp. 1512–1514, Nov. 1981, doi: 10.1109/PROC.1981.12190.
[35] "Introduction to COMSOL multiphysics." COMSOL Multiphysics. 2023. [Online]. Available: https://www.comsol.com
[36] "AC/DC module application gallery examples." Accessed: Mar. 29, 2023. [Online]. Available: https://www.comsol.com/models/acdc-module/page/4
[37] "MatWeb material property data." 2020. [Online]. Available: https://www.matweb.com
[38] S. Hussain, S. A. Ali, T. Islam, and M. R. Mahboob, "Design and detection method of a four electrodes cross-conductive sensor for fluid conductivity measurement," *Appl. Phys. A*, vol. 129, no. 5, p. 314, Apr. 2023, doi: 10.1007/s00339-023-06577-2.
[39] Z. H. Zargar and T. Islam, "A novel cross-capacitive sensor for non-contact microdroplet detection," *IEEE Trans. Ind. Electron.*, vol. 66, no. 6, pp. 4759–4766, Jun. 2019, doi: 10.1109/TIE.2018.2863205.
[40] H. Kamel, D. Abdulah, and J. M. Al-Tuwaijari, "Cancer classification using Gaussian naive Bayes algorithm," in *Proc. Int. Eng. Conf. (IEC)*, Jun. 2019, pp. 165–170, doi: 10.1109/IEC47844.2019.8950650.
[41] "Welcome to Colaboratory—Colaboratory." Accessed: Mar. 9, 2023. [Online]. Available: https://colab.research.google.com
[42] T. Islam, M. Yousuf, and M. Nauman, "A highly precise cross-capacitive sensor for metal debris detection in insulating oil," *Rev. Sci. Instrum.*, vol. 91, no. 2, Feb. 2020, Art. no. 25005. [Online]. Available: https://doi.org/10.1063/1.5139925

SAYED AFZAL ALI (Graduate Student Member, IEEE) received the M.Tech. degree from the Electrical and Electronics Engineering Department, National Institute of Technology Nagaland, Nagaland, India, in 2020.

He is currently an ADF Research Scholar with the Department of Electrical Engineering, Tezpur University, Tezpur, India. His current research interests include sensor and sensing technology, humidity sensor, food quality monitoring sensor, water quality, artificial intelligence, and machine learning.

MD. RAHAT MAHBOOB received the B.Tech. and M.Tech. degrees from Aligarh Muslim University, Aligarh, India, in 2009 and 2012, respectively, and the Ph.D. degree from Jamia Millia Islamia University, New Delhi, India, in 2017.

He is currently working as an Assistant Professor with the Electrical Engineering Department, Tezpur University (Central University), Tezpur, India. His current research interests include thin film sensor, food quality monitoring sensor, wearable sensor, and wireless sensing, IoT, and AI.

TARIKUL ISLAM (Senior Member, IEEE) received the M.Sc. Eng. degree in instrumentation and control system from Aligarh Muslim University, Aligarh, India, in 1997, and the Ph.D. (Eng.) degree from Jadavpur University, Kolkata, India, in 2007.

From 1997 to 2006, he was Assistant Professor and from 2006 to 2012, he was an Associate Professor with the Electrical Engineering Department, Jamia Millia Islamia, a Central University, New Delhi, India, where he has been working as a Professor since 2012. He has over 24 years of teaching and research experiences. He has authored/coauthored ten book chapters, three edited books, filed five Indian patents (two awarded), and published more than 180 papers in peer-reviewed journals and conferences. His research interests include sensing technologies and electronics instrumentation.

Prof. Islam is a Topical Editor of the IEEE SENSORS JOURNAL and an Associate Editor of the IEEE TRANSACTIONS ON INSTRUMENTATION AND MEASUREMENT. He is a Life Member of IETE (India) and ISTE (India).